Membrane Biology:

Human P-glycoprotein Contains a Greasy Ball-and-Socket Joint at the Second Transmission Interface

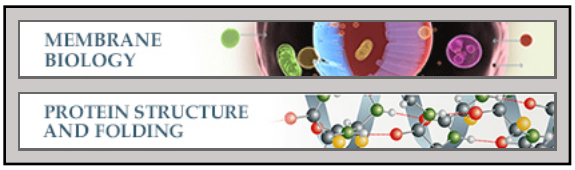

Tip W. Loo, M. Claire Bartlett and David M. Clarke

J. Biol. Chem. *published online June 3, 2013*

Access the most updated version of this article at doi: 10.1074/jbc.M113.484550

Find articles, minireviews, Reflections and Classics on similar topics on the JBC Affinity Sites.

Alerts:

- When this article is cited
- When a correction for this article is posted

Click here to choose from all of JBC's e-mail alerts

This article cites 0 references, 0 of which can be accessed free at
http://www.jbc.org/content/early/2013/06/03/jbc.M113.484550.full.html#ref-list-1

Downloaded from http://www.jbc.org/ at University of Washington on November 6, 2013

JBC Papers in Press. Published on June 3, 2013 as Manuscript M113.484550
The latest version is at http://www.jbc.org/cgi/doi/10.1074/jbc.M113.484550

Human P-glycoprotein Contains a Greasy 'Ball-and-Socket' Joint at the Second Transmission Interface

Tip W. Loo, M. Claire Bartlett, and David M. Clarke
[1]**Department of Medicine and Department of Biochemistry, University of Toronto, Toronto, Ontario. M5S 1A8. Canada**

Running Title: IH2 Mediates TMD/NBD Coupling in the P-gp Drug Pump

Address Correspondence to: David M. Clarke, Department of Medicine, University of Toronto, 1 King's College Circle, Rm. 7342, Medical Sciences Building, Toronto, Ontario. M5S 1A8. Canada. Tel. or FAX: 416-978-1105; E-mail: david.clarke@utoronto.ca

Background: The human P-glycoprotein drug pump confers multidrug resistance.
Results: Hydrophobic suppressors in intracellular loop 2 restored activity to mutants with defective coupling between the ATP- and drug-binding domains.
Conclusion: A greasy 'ball–and-socket' joint connects the ATP- and drug-binding domains.
Significance: Identifies key component of the drug pump mechanism and potential target to modulate this clinically important protein.

The P-glycoprotein (P-gp) drug pump protects us from toxins. Drug-binding sites in the transmembrane (TM) domains (TMDs) are connected to the nucleotide-binding domains (NBDs) by intracellular helices (IHs). TMD-NBD crosstalk is a key step in the transport mechanism since drug binding stimulates ATP hydrolysis followed by drug efflux. Here, we tested whether the IHs are critical for maturation and TMD-NBD coupling by characterizing the effects of mutations to the IH1 and IH2 interfaces. While IH1 mutations had little effect, most mutations at the IH2-NBD2 interface inhibited maturation or activity. For example, the F1086A mutation at the IH2-NBD2 interface abolished drug-stimulated ATPase activity. The mutant F1086A however, retained the ability to bind ATP and drug substrates. The mutant was defective in mediating ATP-dependent conformational changes in the TMDs because binding of ATP no longer promoted cross-linking between cysteines located at the extracellular ends of TM segments 6 and 12. Replacement of Phe1086 (in NBD2) with hydrophobic but not charged residues yielded active mutants. The activity of the F1086A mutant could be restored when the nearby residue Ala266 (in IH2) was replaced with aromatic residues. These results suggest that Phe1086/Ala266 lies in a hydrophobic IH2-NBD2 'ball-and-socket' joint.

ATP binding cassette (ABC) membrane transport proteins couple ATP hydrolysis to the movement of a diverse range of substrates across cell membranes (*1*) They can act as importers, exporters, or extract compounds from the lipid bilayer. A distinguishing feature of ABC proteins is that they contain at least two transmembrane domains (TMDs) with at least 6 transmembrane (TM) segments each and two nucleotide-binding domains (NBDs) that each contains a characteristic LSGGQ (signature) sequence.

Substrates of the 48 human ABC proteins include hydrophobic drugs, bile acids, ions, peptides, nucleosides, sterols, and carbohydrates. Human ABC proteins not only play important physiological roles, but mutations in at least 14 ABC transporter genes have been linked to hereditary diseases (*2*). Diseases include cystic fibrosis, adrenoleukodystrophy, Tangier disease, Dubin–Johnson syndrome Stargardt disease, age-related macular degeneration, and progressive familial intrahepatic cholestasis. Mutations can cause disease by disrupting activity, expression, folding, or trafficking of the proteins. In the case of drug pumps, overexpression can cause multidrug resistance. In addition, drug pumps can

Copyright 2013 by The American Society for Biochemistry and Molecular Biology, Inc.

affect the pharmacokinetics of many drugs and their modulation might also be useful in regulating the bioavailability of drugs (*3*).

The P-glycoprotein drug pump (P-gp, ABCB1) was the first human ABC protein to be discovered during efforts to determine how cancer cells developed multidrug resistance (*4*). P-gp was found to mediate the ATP-dependent efflux of a wide range of hydrophobic compounds (such as anticancer drugs, hydrophobic drugs, steroids, peptides, detergents and lipids) that enter cells by diffusion through the plasma membrane (*5, 6*). P-gp is expressed in the epithelium of liver, kidney, and gastrointestinal tract and at the blood-brain or blood-testes barrier where it functions to protect us from cytotoxic compounds. It is clinically important because it contributes to multidrug resistance in diseases such as cancer and AIDS (*5*). An important goal in P-gp studies is to understand the mechanism of drug efflux and use this knowledge to develop inhibitors aimed at overcoming multidrug resistance.

The 1280 amino acids of human P-gp (*7*) are organized as two tandem repeats of 610 amino acids that are joined by a linker region. Each repeat consists of an NH_2-terminal TMD containing 6 TM segments followed by a NBD. Drug substrates appear to bind at multiple drug-binding sites within a cavity located at the interface between the TMDs (*8-11*). Mg.ATP binds at the interface between the NBDs that interact in a head-to-tail fashion. In this 'nucleotide-sandwich conformation', each nucleotide would interact with the phosphate-binding loop (P-loop) of one NBD and the ABC signature motif (LSGGQ) of the other NBD. ATP hydrolysis occurs by an alternating site mechanism as inhibition of ATPase activity at one site causes a complete loss of ATPase activity (*12-15*).

The mechanism of how hydrolysis of one or two ATP molecules is coupled to drug transport is unknown. It has been proposed that P-gp can exist in at least two major conformations during the catalytic cycle – an inward-facing conformation with separated NBDs and drug-binding sites exposed to the cytoplasm (open conformation) and an outward-facing conformation with close association of the NBDs and drug-binding sites exposed to the extracellular surface (closed conformation) (*16*). Drug substrates and ATP were predicted to induce formation of an outward-facing conformation. Hydrolysis of the first ATP would promote drug transport and hydrolysis of the second ATP would convert the protein back to an inward-facing conformation. Hydrolysis of a second ATP molecule may also contribute to drug transport.

There is a considerable degree of crosstalk between the TMDs and NBDs during the reaction cycle as drug binding activates ATPase activity and ATP hydrolysis leads to drug efflux from the TMDs. An X-ray crystal structure of the P-gp drug pump from *Caenorhabditis elegans (C. elegans)* in an open conformation showed that TMDs were connected to the NBDs by four intracellular helices (IHs) within the intracellular loops (ICLs) that were proposed to act as 'ball-and-socket' joints (*17*). While there is no high-resolution crystal structure of human P-glycoprotein, the *C. elegans* P-gp appeared to be a good model for human P-gp in an open conformation since the structure was more compatible with biochemical studies of the TMDs (*11, 18-21*) and ICL2 (*22*) compared to the crystal structure of mouse P-gp (*8*).

Models of human P-gp in a closed conformation have been built (*23, 24*) using the Sav1866 crystal structure (*25*) as a template. Sav1866 is a homodimeric bacterial ABC drug pump that is predicted to have a similar architecture to human P-gp. It was predicted that the IHs of Sav1866 acted as transmission interfaces to transmit conformational changes associated with ATP binding and hydrolysis at the NBDs to the TMDs (*25*).

In this study, we tested the prediction that the IHs acted as transmission interfaces to link ATP-dependent conformational changes from the NBDs to the TMDs by characterizing IH1 and IH2. IH1 is in an intracellular loop between TM segments 2 and 3 that connects TMD1 to NBD1. IH2 is in an intracellular loop between TM segments 4 and 5 that connects TMD1 to NBD2. IH2 appears to be particularly important because we showed that a cysteine introduced into IH2 (A266C) could be directly cross-linked to a cysteine in NBD2 (F1086C) but the mutant was inactive (*21*). By contrast, cysteine mutations at the equivalent sites at the fourth transmission interface (links IH4 in TMD2 to NBD1) (L443C(NBD1)/S909C(IH4) had no effect on activity (*21*). The IH2-NBD2 contact point also appears to be particularly

important for folding of P-gp because point mutations in IH2 (*26*) and deletion of NBD2 in P-gp but not CFTR (*27*) (P-gp's sister protein) inhibited maturation (*28*).

In this study, we first compared the effects of mutations to IH1 and IH2 on maturation of P-gp. None of the mutations in IH1 inhibited folding or activity of P-gp. By contrast, most mutations to IH2 inhibited P-gp maturation. Since mutant A266C/F1086C was inactive, we characterized the Ala266/Phe1086 interface to determine its role in the transport cycle. We report the identification of a potential 'greasy' hydrophobic ball-and-socket connection at the IH2-NBD2 transmission interface critical for maturation and activity of P-gp.

EXPERIMENTAL PROCEDURES

Expression and Maturation of Mutants – Mutants were constructed to contain a polyhistidine (*29*) or A52 epitope tag at their C-terminal ends for use in whole cell immunoblot assays (*26*). The presence of the epitope tag distinguished the mutant proteins from any endogenous P-gp. P-gp contains three N-linked glycosylation sites can be used to monitor maturation of human P-gp from an immature 150 kDa protein to a mature 170 kDa protein.

Mutations were introduced into the human P-gp cDNA as described previously (*30*). Mutants were expressed in HEK 293 cells for 18 h in the presence or absence of 10 μM cyclosporine A. Expression in the presence of drug substrates like (10 μM) cyclosporine A or (25 μM) verapamil promotes maturation of processing mutants (*31, 32*). Whole cell extracts were subjected to immunoblot analysis using monoclonal antibody A52. The gel lanes were scanned and the amount of mature 170 kDa product relative to total P-gp (immature 150 kDa P-gp plus mature) was analyzed using the NIH Image program and an Apple computer.

Purification of P-gp and Measurement of ATPase Activity – Histidine-tagged P-gps were expressed in HEK 293 cells and then isolated by nickel-chelate chromatography as described previously (*12*). Recovery of P-gp was monitored by immunoblot analysis with rabbit anti-P-gp polyclonal antibody (*12*). A sample of the isolated histidine-tagged P-gp was mixed with an equal volume of 10 mg/ml sheep brain phosphatidylethanolamine (Type II-S, Sigma) that had been washed and suspended in TBS (pH 7.4). ATPase activity was measured in the presence of saturating concentration (0.6 mM) verapamil.

Effect of F1086A on Vanadate Trapping – The double cysteine mutant L443C/S909C was used to test if the F1086A mutation inhibited vanadate trapping of nucleotide. Vanadate trapping inhibits cross-linking of L443C/S909C P-gp (*20*). Membranes prepared from cell expressing L443C/S909C or L443C/S909C/F1086A were incubated in the presence or absence of 5 mM Mg.ATP plus 0.2 mM vanadate for 5 min at 37 ^{o}C. Samples were then treated with 1 mM copper phenanthroline for 15 min at 0 ^{o}C. The reactions were performed using a protein concentration of 0.4 mg/ml. The reactions were stopped by addition of SDS sample buffer (125 mM Tris-HCl, pH 6.8, 20% (v/v) glycerol and 4% (w/v) SDS) containing 5 mM EDTA and no thiol reducing agent. Samples of the reaction mixtures (1 μg protein) were then subjected to SDS-PAGE (6.5% (w/v) polyacrylamide gels; 1.5 mm 15-slot minigels) and immunoblot analysis with a rabbit polyclonal antibody against P-gp. Intramolecular disulfide cross-linking between P-gp domains can be detected because the cross-linked product migrates with a slower mobility on SDS-PAGE gels (*33*).

Effect of Mutations on ATP-Dependent Cross-linking of P-gp Extracellular Segments – Mutant T333C/L975C contains cysteines predicted to reside at the extracellular ends of TM segments 6 and 12, respectively (*30*). The double cysteine T333C/L975C constructs (with or without the F1086A or A266F mutations) were transiently expressed in HEK 293 cells. Membranes were prepared, suspended in TBS, pH 7.4, and treated with 0.5 mM bis(maleimido)ethane (BMOE) in the presence or absence of 5 mM Mg.ATP, 5 mM Mg.ADP, or 5 mM AMP.PNP for 5 min at 20 ^{o}C. The reactions were performed using a protein concentration of 0.4 mg/ml. The reactions were stopped by addition of SDS sample buffer and samples subjected to immunoblot analysis.

Viewing of Structures – The structures of P-gp were viewed using Pymol (*34*).

RESULTS

Mutations in IH2 but not IH1 Inhibit Maturation of P-gp – IH2 (residues Ile261 – Phe267 in cytoplasmic loop 2 (ICL2)) is predicted to connect TMD1 to NBD2 (Fig. 1A) (*17*). TMD1-NBD2 interactions may be particularly important for folding of P-gp into a native structure during synthesis since a ΔNBD2 truncation mutant does not mature (*28*). By contrast, deletion of NBD2 in the CFTR protein which has a similar structure to P-gp (*30*) yielded a mature product (*28*) that was as stable as its full-length counterpart (*27*).

To test if IH2 was important for folding, the effect of mutations to residues Ala259 – Gln270 (IH2 and flanking residues) on maturation was examined. Maturation of P-gp can readily be monitored using immunoblot analysis of whole cell extracts of transfected cells since P-gp is a glycosylated protein. P-gp contains three N-linked glycosylation sites in the extracellular loop that connects TM segments 1 and 2 (Fig. 1A). Mutations that inhibit folding trap P-gp as a 150 kDa core-glycosylated immature protein in the endoplasmic reticulum. Wild-type P-gp undergoes processing in the Golgi to yield a 170 kDa mature protein.

Most of the IH2 mutations (10 of 12) partially or completely inhibited maturation of P-gp (Fig. 1B and C). The I261S, V264S, F267A, G268V, and G269V mutations blocked maturation such that the 150 kDa immature protein was the major product (Fig. 1B). Mutants A259L and A266L were similar to wild-type P-gp as the 170 kDa mature protein was by far the most prominent product. Mutants A260L, R262A, T263A, I265S, and Q270A yielded a mixture of mature and immature P-gp (Fig. 1B and C).

IH1 (residues Ile160 – His166) in ICL1 (connects TM segments 2 and 3) resides at the TMD1-NBD1 interface (Fig. 2A). In contrast to IH2, we found that none of the mutations introduced to IH1 and flanking residues (Gln158-Gly169) substantially inhibited maturation of P-gp (Fig. 2B).

Since IH1 mutations did not affect maturation, we tested whether some of the mutations affected activity. Mutants I160A, G161V, and D164A were selected for analysis because the recent high resolution crystal structure of *C. elegans* P-gp showed that residues at these positions interacted with NBD1 (*17*). The histidine-tagged mutants were expressed in HEK 293 cells, isolated by nickel-chelate chromatography, and assayed for verapamil-stimulated ATPase activity. Verapamil was used because it is transported by P-gp (*35*) and it highly stimulates the ATPase activity of human P-gp (over 10-fold) (*36*). It was found that the activity of all three mutants was similar to that of wild-type P-gp (Fig. 2C).

The F1086A NBD1 Mutation Blocks ATP-Dependent Extracellular Conformation Changes between the TMDs – Models of P-gp in the open and closed conformations are shown (Fig. 3A and B). The major difference between the open and closed conformations is that the NBDs are far apart in the open conformation (Fig. 3A) but in close proximity in the closed conformation (Fig. 3B).

The models shown in Fig. 3A and 3B predict that Ala266 in IH2 would be close to Phe1086 in NBD2. In a previous study, we provided biochemical evidence that Ala266 was indeed close to Phe1086 in NBD2 because mutant A266C/F1086C showed robust cross-linking even when treated with oxidant at 0 ^{o}C to slow molecular motion (*21*). The Ala266/Phe1086 contact point appeared to be critical for function because mutant A266C/F1086C was inactive (*21*). By contrast, introduction of cysteine mutations at the equivalent sites between IH4 (S909C) and NBD1 (L443C) (Fig. 3A and B) had no effect on activity (*21*).

To determine if one or both cysteine mutations in mutant A266C/F1086C inhibited activity, mutants were constructed in a Cys-less background that contained only Cys266 or Cys1086. The mutants were expressed in HEK 293 cells in the presence of the drug substrate cyclosporine A (to promote maturation (*32*)), isolated by nickel-chelate chromatography, and assayed for verapamil-stimulated ATPase activity. It was observed that only the F1086C mutation caused a drastic reduction in verapamil-stimulated ATPase activity (Fig. 3C).

An explanation for the ability of the F1086C mutation to inhibit P-gp activity was that the mutation affected folding of P-gp. To test if the F1086C mutation inhibited folding, the F1086C as well as the Y1087C mutant were expressed in the

absence of drug substrates. The Y1087C mutant was included because an aromatic residue at position 1087 is highly conserved in ABC proteins (*17*). It was found that both the F1086C and Y1087C mutations inhibited maturation of Cys-less P-gp (Fig. 3D).

There are subtle differences in the activity of Cys-less P-gp compared to the wild-type protein (*37*). In addition, it was possible that replacement of Phe1086 with a cysteine caused a defect in the structure of P-gp that would be different if it had been replaced with a smaller amino acid. To test if replacement of Phe1086 with a small amino acid would affect maturation, mutants F1086A or Y1087A in the wild-type background were constructed and expressed in HEK 293 cells. Fig. 3D shows that the Y1087A but not the F1086A mutation inhibited P-gp maturation (Fig. 3D). Although the F1086A mutation did not inhibit folding, it still inhibited verapamil-stimulated ATPase activity (Fig. 3C).

Why do changes to Phe1086 inhibit P-gp verapamil-stimulated ATPase activity? To address this question, we first tested whether the F1086A mutation blocked interactions with ATP or verapamil.

It is possible that mutations to Phe1086 could affect ATP interactions since the residue is close to the Walker A site in NBD2 (residues Ser1077 to Gly1084). To test if mutant F1086A retained the ability to bind and hydrolyze ATP, we tested whether vanadate trapping of ATP would still inhibit cross-linking of mutant F1086A/L443C/S909C. P-gp can be trapped at a transition state during ATP hydrolysis by including vanadate in the reaction mix (35). Vanadate traps ADP at either NBD by mimicking the transition state of the γ-phosphate of ATP during hydrolysis and trapping at one NBD inhibits ATP hydrolysis at the second site (35). Vanadate trapping of nucleotide causes conformational changes in P-gp and this can be detected by disulfide cross-linking analysis (36). For example, vanadate trapping of nucleotide inhibits cross-linking of mutant L443C(NBD1)/S909C(IH4) (*21*). Accordingly, membranes prepared from cells expressing mutant F1086A/L443C(NBD1)/S909C(IH4) were preincubated with or without ATP plus vanadate for 5 min at 37 °C. Samples were then cooled on ice, treated with copper phenanthroline and subjected to immunoblot analysis. Fig. 3E shows that vanadate trapping of nucleotide blocked cross-linking in both mutants L443C(NBD1)/S909C(IH4) and L443C(NBD1)/S909C(IH4)/F1086A. These results show that the F1086A mutation did not inhibit ATP hydrolysis.

A drug-rescue assay was then used to test if the F1086A mutation disrupted verapamil interactions with the TMDs. The rationale of the drug-rescue assay is that expression of a P-gp processing mutant in the presence of verapamil will promote maturation if the mutant retains the ability to bind verapamil (*32*). Mutations that disrupt the verapamil-binding site will prevent rescue of processing mutants with verapamil (*21*). Accordingly, the F1086A mutation was introduced into the P709A processing mutant. The P709A mutant was selected because the mutation is located in the linker region that connects the two halves of P-gp and is outside the ATP- and drug-binding sites (Figs. 3A and 3B). Expression of mutant P709A/F1086A yielded the 150kDa immature form of P-gp as the major product (Fig. 3F). The mutant retained the ability to bind verapamil however, because the mutant was rescued when expressed in the presence of verapamil such that the 170 kDa mature form of P-gp was the major protein product (Fig. 3F).

It is possible that the F1086A mutation inhibited activity by disrupting coupling between the NBDs and TMDs. Accordingly, cross-linking of mutant T333C/L975C was used to test the effect of F1086A on coupling. The T333C and L975C mutations are located at the extracellular ends of TM segments 6 and 12, respectively (Fig. 3A and B). Mutant T333C/L975C can be cross-linked when intact cells expressing the mutant are treated with BMOE cross-linker (*30*). Mutant T333C/L975C however, does not show cross-linking if membranes containing the mutant are treated only with BMOE (Fig. 4A). This suggested that ATP was required for cross-linking. Therefore, cross-linking of the mutant in membranes was carried out in the presence of ATP and other nucleotides. Fig. 4A shows that binding of ATP is required because cross-linking was observed in the presence of ATP or the non-hydrolyzable ATP analog AMP.PNP, but not in the presence of ADP (Fig. 4A). These results suggest that binding of ATP is coupled to a

conformational change at the extracellular regions of P-gp that orients cysteines at 333(TM6) and 975(TM12) in positions that can be cross-linked with BMOE.

To determine if the F1086A mutation affected NBD/TMD coupling, it was introduced into mutant T333C/L975C and subjected to cross-linking. It was observed that the F1086A mutation inhibited ATP-dependent cross-linking of the mutant T333C/L975C (Fig. 4B). These results suggest that F1086A disrupted NBD/TMD coupling.

Replacement of Phe1086 with Bulky Hydrophobic Amino Acids Yields Active Mutants – Mutant F1086A was inactive (Fig. 3C). To test if Phe1086 was essential for activity, mutants were constructed such that Phe was replaced with a bulky hydrophobic (Tyr, Leu, Trp) or charged (Asp, Arg) amino acid. Fig. 5A shows that the F1086D or F1086R mutations inhibited maturation of P-gp. By contrast, those containing hydrophobic residues (F1086Y, F1086L, or F1086W) mutations did not inhibit maturation. Mutants F1086D and F1086R could still be rescued if they were expressed in the presence of a drug substrate (Fig. 5B).

The histidine-tagged mutants were then purified and assayed for verapamil-stimulated ATPase activity. Mutants F1086D and F1086R were firsrt expressed in the presence of cyclosporine A to promote maturation before isolating the histidine-tagged protein. It was observed that replacement of Phe1086 with hydrophobic amino acids (Tyr, Leu, Trp) yielded active mutants whereas replacement with charged amino acids yielded mutants with little activity (less than 10% of wild-type P-gp) (Fig. 5C). These results suggest that Phe1086 can be replaced with a hydrophobic amino acid to yield a protein that matures to yield an active molecule.

Replacement of Ala266 with Hydrophobic Residues Restores Activity of Mutant Phe1086A – Models (Fig. 3A and B) and cross-linking results (*21*) predict that Ala266 in IH2 is close to Phe1086 in NBD2. Since a large hydrophobic amino acid might be required at the Ala266/ Phe1086 interface for activity, we tested if replacement of Ala266 with the aromatic amino acids Tyr, Phe or Trp could act as suppressor mutations to restore activity of the F1086A. We also predicted that replacement of Ala266 with a small charged amino acid (Asp) would not restore activity to F1086A. It was found that replacement of Ala266 with aromatic amino acids (A266Y, A266F or A266W) in the F1086A background yielded mature 170 kDa P-gp as the major product (Fig. 6A). By contrast, mutant A266D/F1086A did not mature although it could be rescued when expressed in the presence of cyclosporine A (Fig. 6B).

The histidine-tagged mutants were then isolated and assayed for verapamil-stimulated ATPase activity. Mutant A266D/F1086A was first expressed in the presence of cyclosporine A to promote maturation before isolating the histidine-tagged protein. Fig. 6C shows that the verapamil-stimulated ATPase activities of mutants A266Y/F1086A, A266F/F1086A and A266W/F1086A were similar to that of wild-type P-gp. Mutant A266D/F1086A showed little activity (Fig. 6C). The results show that the aromatic replacements to Ala266 acted as second-site suppressor mutations to restore activity of F1086A.

Replacement of Ala266 with an aromatic amino acid might rescue defective TMD/NBD coupling and thereby restore activity to F1086A. Accordingly, the A266F mutation was introduced into mutant F1086A/T333C/L975C to test if it affected cross-linking between the TMDs. It was found that the A266F mutation restored ATP-dependent BMOE cross-linking of the mutant (Fig. 6D).

DISCUSSION

The results show that IH2 is particularly important for folding of P-gp and coupling between the ATP- and drug-binding domains. For example IH2 appears to be more important than IH1 for promoting TMD1 interactions with the NBDs during synthesis. Most point mutations to IH2 reduced P-gp maturation efficiency (Fig. 1B) whereas none of the point mutations to IH1 inhibited maturation of P-gp (Fig. 2B). Comparison of P-gp to bacterial ABC transporters suggest that it might be expected that mutations to IH2 would have a greater effect on P-gp maturation than IH1 mutations because IH1-

NBD1 interactions are not required for activity or synthesis of many bacterial ABC proteins (*38*).

A dynamic simulation study of human P-gp predicted that IH2-NBD2 interactions would be more important in driving the necessary conformational changes compared to IH1 (*39*). It was found that IH2 made many more contacts with the NBDs compared to IH1. It was also found that IH2 only interacted with NBD2 whereas IH1 contacted both the NBD1 and NBD2 domains. The crystal structure of Sav1866 (homodimer) in a closed conformation also showed that IH2 only contacted an NBD in the opposite subunit whereas IH1 made contact with the NBDs of both subunits (*25*). The crystal structure of *C. elegans* P-gp represents a snapshot of the protein in an open conformation with IH1 only in contact with NBD1 (*17*).

The recent crystal structure of P-gp from *C. elegans* also suggests that the contact between IH2-NBD2 is more important than between IH1-NBD1 (*17*). Only three amino acids in the IH1 region interacted with NBD1 whereas 14 amino acids were identified in the IH2 region (Glu256 – Glu297, equivalent to amino acids to Glu256 – Glu273 in human P-gp) that interacted with NBD2 via salt bridges, hydrogen bonds or van der Waals interactions.

The results may also explain the puzzling difference between maturation of NBD2 deletion mutants of P-gp and its sister protein, CFTR. P-gp and CFTR are both ABC proteins predicted to have similar structures (*30*). Deletion of NBD2 in P-gp inhibits P-gp maturation while deletion of NBD2 in CFTR does not. This study shows that P-gp maturation is highly sensitive to point mutations introduced at the TMD1/NBD2 interface. Most of the mutations introduced into IH2 inhibited maturation of the protein. Detailed analysis of the effect of IH2 mutations in CFTR have not yet been performed. Preliminary studies on the effects of ICL1 and ICL2 mutations in CFTR that cause cystic fibrosis have shown that the ICL1 mutations have more inhibitory effects on CFTR function (*40*).

The presence of hydrophobic amino acids at the ICL2-ND2 interface appears to be critical for P-gp maturation and activity. Fig. 7 shows the locations of amino acids that when mutated, inhibited maturation and/or activity of P-gp. At least some of the mutations to the hydrophobic residues at Tyr1087 or Phe1086 in NBD2 or to hydrophobic residues at Ile261, Val264, Ala266, or Phe267 in IH2 inhibited maturation. Accordingly, we propose that a 'greasy' hydrophobic IH2-NBD2 interface is critical for P-gp maturation and function. All of these residues, with the exception of Ile261, were shown to participate in IH2-NBD2 interactions through hydrogen bonds or van der Waals interactions in the *C. elegans* crystal structure (*17*). It is possible that Ile261 may be involved in contacts at another stage of the reaction or folding steps.

The effects of mutations to Ala266 and Phe1086 suggests that the presence of a hydrophobic interface between IH2 and NBD2 is also important for coupling of ATP interactions with the NBDs to conformational changes in the TMDs. Removal of Phe1086 by mutation to alanine or replacement with charged amino acids inhibited activity and uncoupled ATP binding to conformational changes in the TMDs. Mutants were active if Phe1086 was replaced with a hydrophobic amino acid. In addition, activity of the F1086A mutant could be restored if Ala266 was replaced with an aromatic amino acid. Perhaps the presence of a greasy interface allows rotations of IH2 in the NBD2 cleft.

Studies of multiple crystal structures of the bacterial ABC maltose transporter suggest that its reaction cycle is accompanied by rotation of IH segments within the cleft of the NBDs (*41*). In addition, mutations to the IH-NBD interfaces disrupted activity and structure of the protein (*42*).

In summary, we identified a key hydrophobic interface between IH2 in TMD1 and NBD2. The interface is important for folding into a native structure during synthesis of the P-gp drug pump. The results also support the prediction that IH2-NBD2 site forms a ball-and-socket joint (*17*) that acts as a transmission interface (*25*) to couple the conformational changes associated with binding of ATP and drug substrates.

FOOTNOTES

The abbreviations used are: ABC, ATP-binding cassette; BMOE, bis(maleimido)ethane; *C. elegans*, *Caenorhabdititis elegans*; P-gp, P-glycoprotein; NBD, nucleotide-binding domain; HEK, human embryonic kidney; TM, transmembrane; TMD, transmembrane domain; ICL, intracellular loop; IH, intracellular helix.

ACKNOWLEDGMENTS

This work was supported by grants from the Canadian Institutes of Health Research and the Canadian Cancer Society. DMC is the recipient of the Canada Research Chair in Membrane Biology.

REFERENCES

1. Rees, D. C., Johnson, E., and Lewinson, O. (2009) ABC transporters: the power to change. *Nat Rev Mol Cell Biol 10*, 218-227.
2. Kaminski, W. E., Piehler, A., and Wenzel, J. J. (2006) ABC A-subfamily transporters: structure, function and disease. *Biochim Biophys Acta 1762*, 510-524.
3. Schinkel, A. H., Mayer, U., Wagenaar, E., Mol, C. A., van Deemter, L., Smit, J. J., van der Valk, M. A., Voordouw, A. C., Spits, H., van Tellingen, O., Zijlmans, J. M., Fibbe, W. E., and Borst, P. (1997) Normal viability and altered pharmacokinetics in mice lacking mdr1-type (drug-transporting) P-glycoproteins. *Proc. Natl. Acad. Sci. U. S. A. 94*, 4028-4033.
4. Juliano, R. L., and Ling, V. (1976) A surface glycoprotein modulating drug permeability in Chinese hamster ovary cell mutants. *Biochim. Biophys. Acta 455*, 152-162.
5. Ambudkar, S. V., Dey, S., Hrycyna, C. A., Ramachandra, M., Pastan, I., and Gottesman, M. M. (1999) Biochemical, cellular, and pharmacological aspects of the multidrug transporter. *Annu. Rev. Pharmacol. Toxicol. 39*, 361-398.
6. Eckford, P. D., and Sharom, F. J. (2009) ABC efflux pump-based resistance to chemotherapy drugs. *Chem. Rev. 109*, 2989-3011.
7. Chen, C. J., Chin, J. E., Ueda, K., Clark, D. P., Pastan, I., Gottesman, M. M., and Roninson, I. B. (1986) Internal duplication and homology with bacterial transport proteins in the mdr1 (P-glycoprotein) gene from multidrug-resistant human cells. *Cell 47*, 381-389.
8. Aller, S. G., Yu, J., Ward, A., Weng, Y., Chittaboina, S., Zhuo, R., Harrell, P. M., Trinh, Y. T., Zhang, Q., Urbatsch, I. L., and Chang, G. (2009) Structure of P-glycoprotein reveals a molecular basis for poly-specific drug binding. *Science 323*, 1718-1722.
9. Dey, S., Ramachandra, M., Pastan, I., Gottesman, M. M., and Ambudkar, S. V. (1997) Evidence for two nonidentical drug-interaction sites in the human P-glycoprotein. *Proc. Natl. Acad. Sci. U. S. A. 94*, 10594-10599.
10. Lugo, M. R., and Sharom, F. J. (2005) Interaction of LDS-751 with P-glycoprotein and mapping of the location of the R drug binding site. *Biochemistry 44*, 643-655.
11. Loo, T. W., Bartlett, M. C., and Clarke, D. M. (2009) Identification of residues in the drug-translocation pathway of the human multidrug resistance P-glycoprotein by arginine mutagenesis. *J. Biol. Chem. 284*, 24074-24087.

12. Loo, T. W., and Clarke, D. M. (1995) Covalent modification of human P-glycoprotein mutants containing a single cysteine in either nucleotide-binding fold abolishes drug-stimulated ATPase activity. *J. Biol. Chem. 270*, 22957-22961.
13. Sauna, Z. E., Kim, I. W., Nandigama, K., Kopp, S., Chiba, P., and Ambudkar, S. V. (2007) Catalytic cycle of ATP hydrolysis by P-glycoprotein: evidence for formation of the E.S reaction intermediate with ATP-gamma-S, a nonhydrolyzable analogue of ATP. *Biochemistry 46*, 13787-13799.
14. Delannoy, S., Urbatsch, I. L., Tombline, G., Senior, A. E., and Vogel, P. D. (2005) Nucleotide binding to the multidrug resistance P-glycoprotein as studied by ESR spectroscopy. *Biochemistry 44*, 14010-14019.
15. Urbatsch, I. L., Sankaran, B., Weber, J., and Senior, A. E. (1995) P-glycoprotein is stably inhibited by vanadate-induced trapping of nucleotide at a single catalytic site. *J. Biol. Chem. 270*, 19383-19390.
16. Gutmann, D. A., Ward, A., Urbatsch, I. L., Chang, G., and van Veen, H. W. (2010) Understanding polyspecificity of multidrug ABC transporters: closing in on the gaps in ABCB1. *Trends Biochem Sci 35*, 36-42.
17. Jin, M. S., Oldham, M. L., Zhang, Q., and Chen, J. (2012) Crystal structure of the multidrug transporter P-glycoprotein from Caenorhabditis elegans. *Nature 490*, 566-569.
18. Loo, T. W., Bartlett, M. C., and Clarke, D. M. (2004) Val133 and Cys137 in transmembrane segment 2 are close to residues Arg935 and Gly939 in transmembrane segment 11 of human P-glycoprotein. *J. Biol. Chem. 279*, 18232-18238.
19. Loo, T. W., Bartlett, M. C., and Clarke, D. M. (2006) Transmembrane segment 1 of human P-glycoprotein contributes to the drug binding pocket. *Biochem. J. 396*, 537-545.
20. Loo, T. W., Bartlett, M. C., and Clarke, D. M. (2007) Suppressor mutations in the transmembrane segments of P-glycoprotein promote maturation of processing mutants and disrupt a subset of drug-binding sites. *J. Biol. Chem. 282*, 32043-32052.
21. Loo, T. W., Bartlett, M. C., and Clarke, D. M. (2008) Arginines in the first transmembrane segment promote maturation of a P-glycoprotein processing mutant by hydrogen bond interactions with tyrosines in transmembrane segment 11. *J. Biol. Chem. 283*, 24860-24870.
22. Loo, T. W., and Clarke, D. M. (2013) A Salt Bridge in Intracellular Loop 2 is Essential for Folding of Human P-glycoprotein. *Biochemistry 52*, 3194-3196.
23. Ravna, A. W., Sylte, I., and Sager, G. (2007) Molecular model of the outward facing state of the human P-glycoprotein (ABCB1), and comparison to a model of the human MRP5 (ABCC5). *Theor. Biol. Med. Model. 4*, 33.
24. Globisch, C., Pajeva, I. K., and Wiese, M. (2008) Identification of Putative Binding Sites of P-glycoprotein Based on its Homology Model. *ChemMedChem. 3*, 280-295.
25. Dawson, R. J., and Locher, K. P. (2006) Structure of a bacterial multidrug ABC transporter. *Nature 443*, 180-185.
26. Loo, T. W., and Clarke, D. M. (1994) Functional consequences of glycine mutations in the predicted cytoplasmic loops of P-glycoprotein. *J. Biol. Chem. 269*, 7243-7248.
27. Cui, L., Aleksandrov, L., Chang, X. B., Hou, Y. X., He, L., Hegedus, T., Gentzsch, M., Aleksandrov, A., Balch, W. E., and Riordan, J. R. (2007) Domain Interdependence in the Biosynthetic Assembly of CFTR. *J. Mol. Biol. 365*, 981-994.
28. Wang, Y., Loo, T. W., Bartlett, M. C., and Clarke, D. M. (2007) Modulating the folding of P-glycoprotein and cystic fibrosis transmembrane conductance regulator truncation mutants with pharmacological chaperones. *Mol. Pharmacol. 71*, 751-758.

29. Loo, T. W., and Clarke, D. M. (1995) Rapid purification of human P-glycoprotein mutants expressed transiently in HEK 293 cells by nickel-chelate chromatography and characterization of their drug-stimulated ATPase activities. *J. Biol. Chem. 270*, 21449-21452.
30. Loo, T. W., Bartlett, M. C., Detty, M. R., and Clarke, D. M. (2012) The ATPase activity of the P-glycoprotein drug pump is highly activated when the N-terminal and central regions of the nucleotide-binding domains are linked closely together. *J Biol Chem 287*, 26806-26816.
31. Loo, T. W., and Clarke, D. M. (1999) The transmembrane domains of the human multidrug resistance P-glycoprotein are sufficient to mediate drug binding and trafficking to the cell surface. *J. Biol. Chem. 274*, 24759-24765.
32. Loo, T. W., and Clarke, D. M. (1997) Correction of defective protein kinesis of human P-glycoprotein mutants by substrates and modulators. *J. Biol. Chem. 272*, 709-712.
33. Loo, T. W., Bartlett, M. C., and Clarke, D. M. (2003) Substrate-induced conformational changes in the transmembrane segments of human P-glycoprotein. Direct evidence for the substrate-induced fit mechanism for drug binding. *J. Biol.Chem. 278*, 13603-13606.
34. DeLano, W. L. (2002) The PyMol Molecular Graphics System *DeLano Scientific, Palo Alto, CA. USA.* , <http://www.pymol.org>
35. Omote, H., and Al-Shawi, M. K. (2002) A novel electron paramagnetic resonance approach to determine the mechanism of drug transport by P-glycoprotein. *J. Biol. Chem. 277*, 45688-45694.
36. Loo, T. W., Bartlett, M. C., and Clarke, D. M. (2003) Methanethiosulfonate derivatives of rhodamine and verapamil activate human P-glycoprotein at different sites. *J. Biol. Chem. 278*, 50136-50141.
37. Taylor, A. M., Storm, J., Soceneantu, L., Linton, K. J., Gabriel, M., Martin, C., Woodhouse, J., Blott, E., Higgins, C. F., and Callaghan, R. (2001) Detailed characterization of cysteine-less P-glycoprotein reveals subtle pharmacological differences in function from wild-type protein. *Br J Pharmacol 134*, 1609-1618.
38. Oldham, M. L., Davidson, A. L., and Chen, J. (2008) Structural insights into ABC transporter mechanism. *Curr. Opin. Struct. Biol. 18*, 726-733.
39. Wise, J. G. (2012) Catalytic transitions in the human MDR1 P-glycoprotein drug binding sites. *Biochemistry 51*, 5125-5141.
40. Seibert, F. S., Jia, Y., Mathews, C. J., Hanrahan, J. W., Riordan, J. R., Loo, T. W., and Clarke, D. M. (1997) Disease-associated mutations in cytoplasmic loops 1 and 2 of cystic fibrosis transmembrane conductance regulator impede processing or opening of the channel. *Biochemistry 36*, 11966-11974.
41. Khare, D., Oldham, M. L., Orelle, C., Davidson, A. L., and Chen, J. (2009) Alternating access in maltose transporter mediated by rigid-body rotations. *Mol. Cell 33*, 528-536.
42. Mourez, M., Hofnung, M., and Dassa, E. (1997) Subunit interactions in ABC transporters: a conserved sequence in hydrophobic membrane proteins of periplasmic permeases defines an important site of interaction with the ATPase subunits. *EMBO J 16*, 3066-3077.

FIGURE LEGENDS

Fig. 1. Point mutations to IH2 inhibit P-gp maturation. A) Model of P-gp showing the location of coupling helix IH2 between TMD1 and NBD2. The branched lines represent the glycosylation sites. B) Wild-type and P-gp mutants (mutations to IH2 and flanking regions) were expressed in HEK 293 cells and whole cell SDS extracts subjected to immunoblot analysis. The positions of mature (170 kDa) and immature (150 kDa) forms of P-gp are shown. C) Percent mature is amount of mature protein relative to total P-gp. Each value is the mean $\pm$ S.D obtained from three different transfections.

Fig. 2. Point mutations to IH1 do not inhibit P-gp maturation. A) The location of coupling helix IH1 between TMD1 and NBD1 is shown in the model. B) Whole cell SDS extracts of HEK 293 cells expressing wild-type P-gp and P-gp mutants (mutations to IH1 and flanking regions) were subjected to immunoblot analysis. The positions of mature (170 kDa) and immature (150 kDa) forms of P-gp are shown. C) Verapamil-stimulated ATPase activities of wild-type P-gp and mutants predicted to form contacts between IH1 and NBD1 in the *C. elegans* P-gp crystal structure (*17*). The results are the mean of three different transfections $\pm$ S.D.

Fig. 3. Mutations to Phe1086 inhibit P-gp activity. Structure of P-gp in the open (A) (*17*) or closed (B) (*24*) conformations are shown. C) Histidine-tagged Cys-less P-gp or mutants A266C/F1086C, A266C, and F1086C (in Cys-less background) as well as wild-type P-gp and mutant F1086A (in wild-type background) were isolated and ATPase activities measured in the presence of verapamil. Each value is the mean $\pm$ S.D. (n=3). D) Whole cell SDS extracts of cells expressing P-gp mutants (in Cys-less or wild-type background) were subjected to immunoblot analysis. The positions of mature (170 kDa) and immature (150 kDa) forms of P-gp are indicated. E) Membranes prepared from cells expressing L443C/S909C $\pm$ F1086A were first treated with (+VO_4) or without (-VO_4) Mg.ATP plus vanadate. Samples were then treated with (+) or without (-) copper phenanthroline (CuP) and subjected to immunoblot analysis. The positions of the cross-linked (X-link) and mature (170 kDa) P-gps are indicated. F) The P709A processing mutation was introduced into mutant F1086A. Mutants were expressed in the presence (+) or absence (-) of verapamil (Ver) and whole cell extracts subjected to immunoblot analysis.

Fig. 4. F1086A inhibits ATP-dependent cross-linking at the extracellular surface. Membranes prepared from cells expressing mutant T333C/L975C (A) or T333C/L975C/F1086A (B) were treated with BMOE in the absence (None) or presence of nucleotides (ATP, AMP.PNP or ADP). Samples were subjected to immunoblot analysis. The positions of the cross-linked (X-link) and mature (170 kDa) P-gps are indicated.

Fig. 5. P-gp matures and retains activity when Phe1086 is replaced with hydrophobic but not charged residues. A) Phe1086X mutants were expressed in the absence of drug substrates. B) Processing mutants F1086D and F1086R were expressed in the presence (+) or absence (-) of cyclosporine A (Cyclo) and whole cell SDS extracts were subjected to immunoblot analysis. The positions of mature (170 kDa) and immature (150 kDa) P-gps are indicated. C) ATPase activities of histidine-tagged wild-type P-gp and Phe1086X mutants were measured in the presence of verapamil. Histidine-tagged mutants F1086D and F1086R were first expressed in the presence of

cyclosporine A to promote maturation of P-gp before isolation of the protein by nickel-chelate chromatography. Each value is the mean ± S.D. (n=3).

Fig. 6. Replacement of Ala266 with aromatic residues restores F1086A activity. A) Wild-type P-gp or Ala266X mutants containing the F1086A mutation were expressed in the absence of drug substrates. B) Mutant A266D/F1086A was expressed in the presence (+) or absence (-) of cyclosporine A (Cyclo). Samples (from A or B) were subjected to immunoblot analysis. The positions of mature (170 kDa) and immature (150 kDa) P-gps are indicated. C) ATPase activities of wild-type P-gp and F1086A mutants containing replacements to Ala266 were measured in the presence of verapamil. Mutant A266D was first expressed in the presence of cyclosporine A before isolation of the protein by nickel-chelate chromatography. Each value is the mean ± S.D. (n=3). D) Membranes prepared from cells expressing mutants T333C/L975C (None), T333C/L975C/F1086A, or T333C/L975C/F1086A/A266F were treated with BMOE in the presence (+) or absence (-) of ATP. Samples were subjected to immunoblot analysis. The positions of cross-linked (X-link) and mature (170 kDa) P-gps are indicated.

Fig. 7. Model showing hydrophobic amino acids at the IH2-NBD2 interface critical for P-gp maturation and/or activity. Residues Val253 – Asn278 (ICL2) and Val1080 – Pro1089 (NBD2) are shown. The locations of residues Ile261, Val264, Phe267, and Tyr1087 are shown as mutation to these residues inhibited maturation. Removal of the aromatic side chain of Phe1086 (F1086A mutation) inhibited P-gp activity because it inhibited coupling between the ATP- and drug-binding domains. Replacement of Ala266 with aromatic residues restored the activity of F1086A. Residues Glu256 and Arg276 were recently shown to form a salt bridge that was critical for P-gp maturation (*22*).

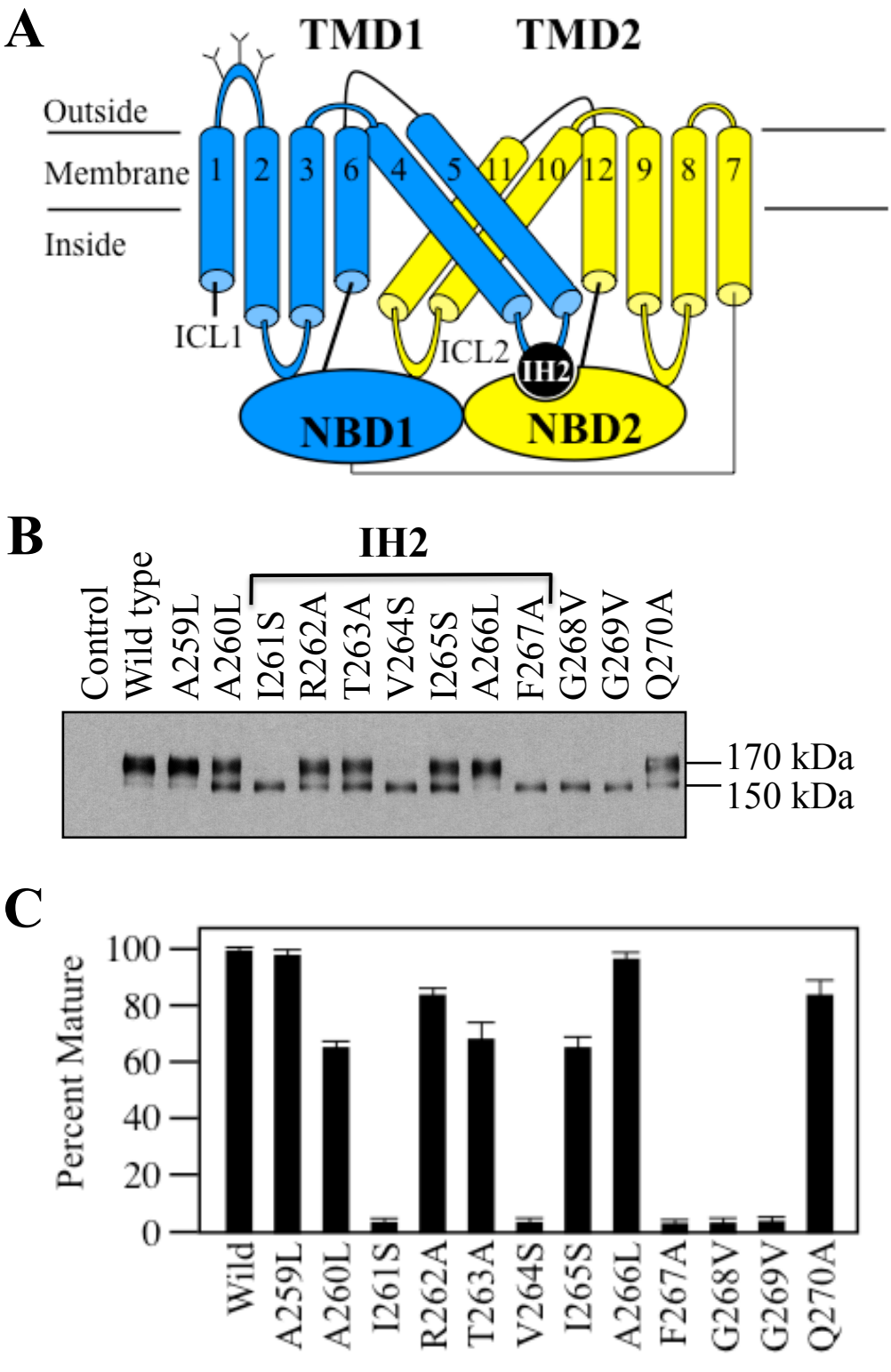
A
TMD1
TMD2
Outside
Membrane
Inside
1
2
3
6
4
5
11
10
12
9
8
7
ICL1
ICL2
IH2
NBD1
NBD2
B
IH2
Control
Wild type
A259L
A260L
I261S
R262A
T263A
V264S
I265S
A266L
F267A
G268V
G269V
Q270A
170 kDa
150 kDa
C
Percent Mature
100
80
60
40
20
0
Wild
A259L
A260L
I261S
R262A
T263A
V264S
I265S
A266L
F267A
G268V
G269V
Q270A

Fig. 1

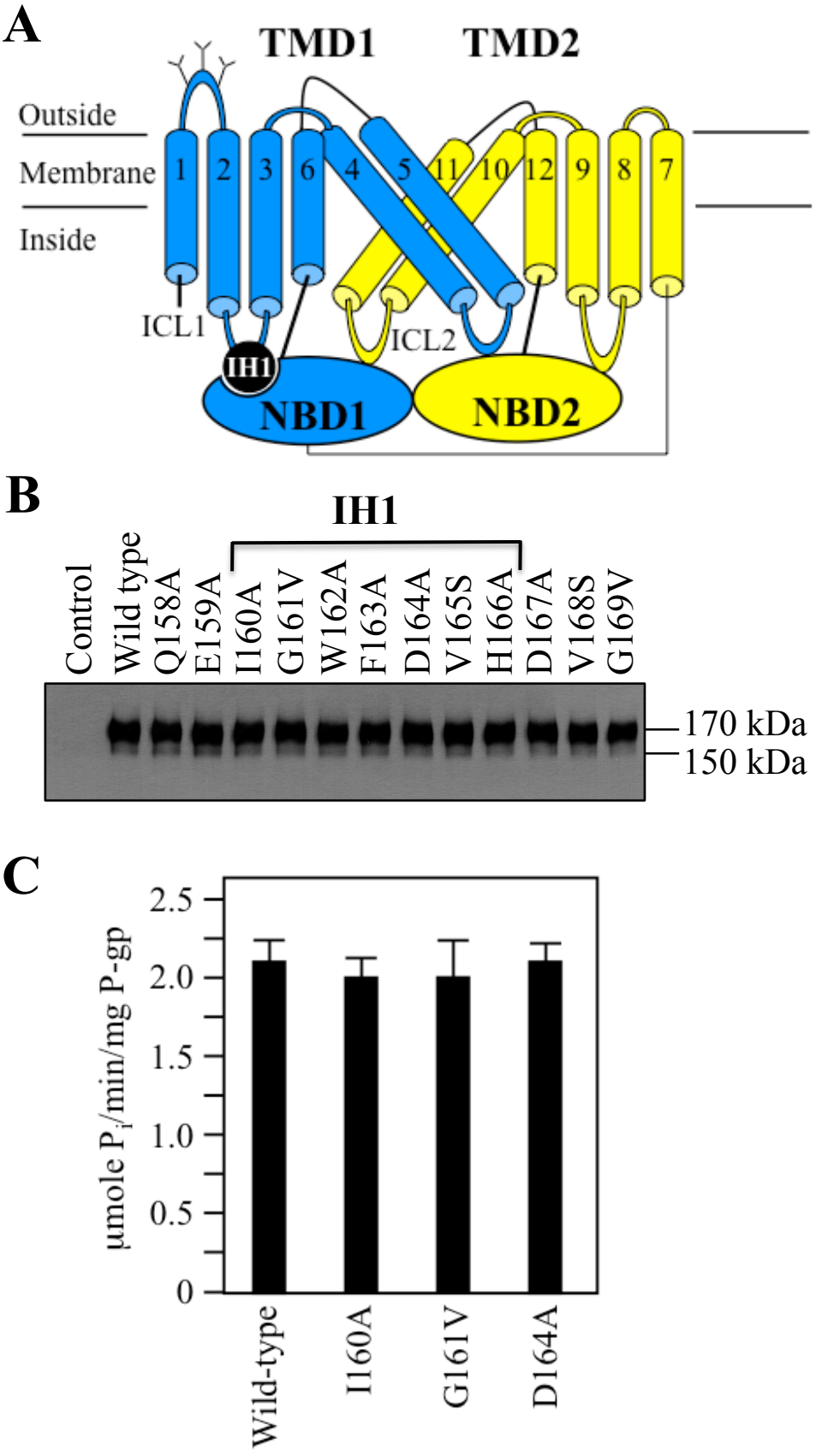
A
TMD1
TMD2
Outside
Membrane
Inside
1
2
3
6
4
5
11
10
12
9
8
7
ICL1
ICL2
IH1
NBD1
NBD2
B
IH1
Control
Wild type
Q158A
E159A
I160A
G161V
W162A
F163A
D164A
V165S
H166A
D167A
V168S
G169V
170 kDa
150 kDa
C
μmole Pi/min/mg P-gp
2.5
2.0
1.5
1.0
0.5
0
Wild-type
I160A
G161V
D164A

Fig. 2

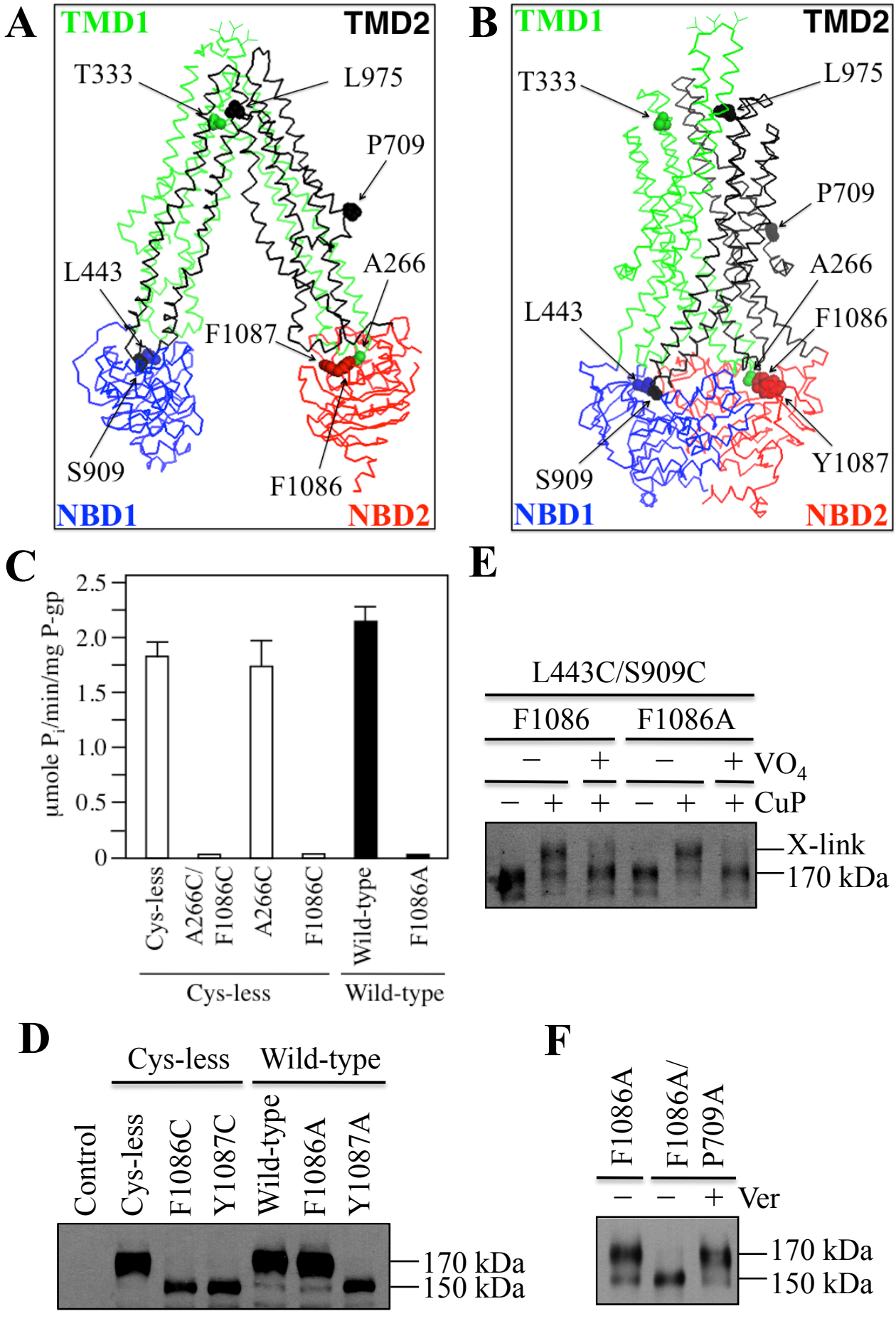
A
TMD1
TMD2
T333
L975
P709
L443
A266
F1087
S909
F1086
NBD1
NBD2
B
TMD1
TMD2
T333
L975
P709
A266
L443
F1086
S909
Y1087
NBD1
NBD2
C
μmole Pi/min/mg P-gp
2.5
2.0
1.5
1.0
0.5
0
Cys-less
A266C/ F1086C
A266C
F1086C
Wild-type
F1086A
Cys-less
Wild-type
E
L443C/S909C
F1086
F1086A
− + − + VO4
− + + − + + CuP
X-link
170 kDa
D
Cys-less
Wild-type
Control
Cys-less
F1086C
Y1087C
Wild-type
F1086A
Y1087A
170 kDa
150 kDa
F
F1086A
F1086A/ P709A
− − + Ver
170 kDa
150 kDa

Fig. 3

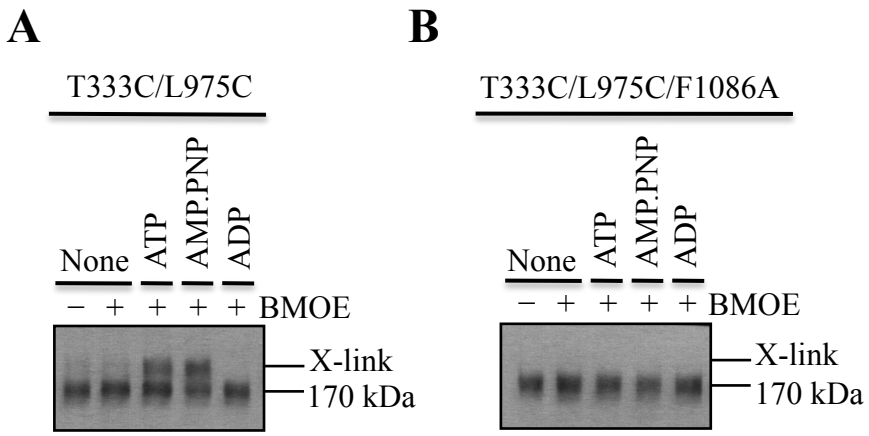
A
T333C/L975C
None
ATP
AMP.PNP
ADP
− + + + + BMOE
X-link
170 kDa
B
T333C/L975C/F1086A
None
ATP
AMP.PNP
ADP
− + + + + BMOE
X-link
170 kDa

Fig. 4

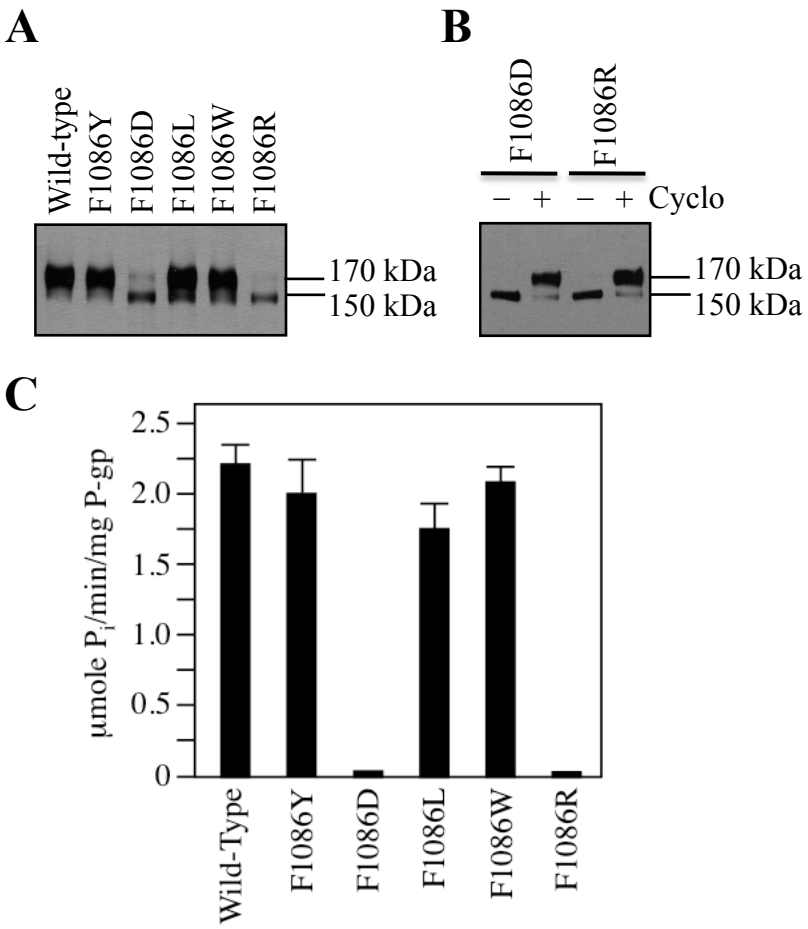
A
Wild-type
F1086Y
F1086D
F1086L
F1086W
F1086R
170 kDa
150 kDa
B
F1086D
F1086R
– + – + Cyclo
170 kDa
150 kDa
C
μmole Pi/min/mg P-gp
2.5
2.0
1.5
1.0
0.5
0
Wild-Type
F1086Y
F1086D
F1086L
F1086W
F1086R

Fig. 5

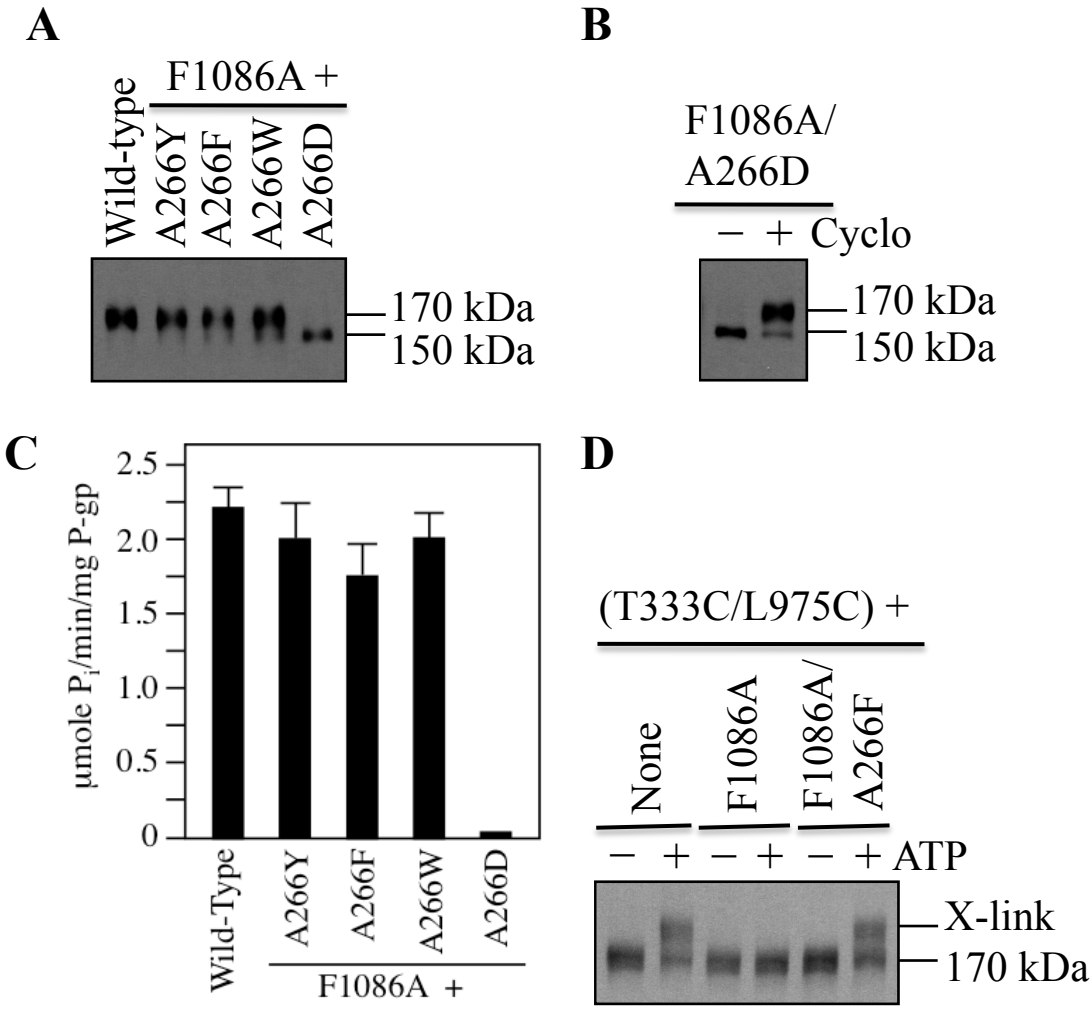
A
F1086A +
Wild-type
A266Y
A266F
A266W
A266D
170 kDa
150 kDa
B
F1086A/
A266D
– + Cyclo
170 kDa
150 kDa
C
μmole Pi/min/mg P-gp
2.5
2.0
1.5
1.0
0.5
0
Wild-Type
A266Y
A266F
A266W
A266D
F1086A +
D
(T333C/L975C) +
None
F1086A
F1086A/
A266F
– + – + – + ATP
X-link
170 kDa

Fig. 6

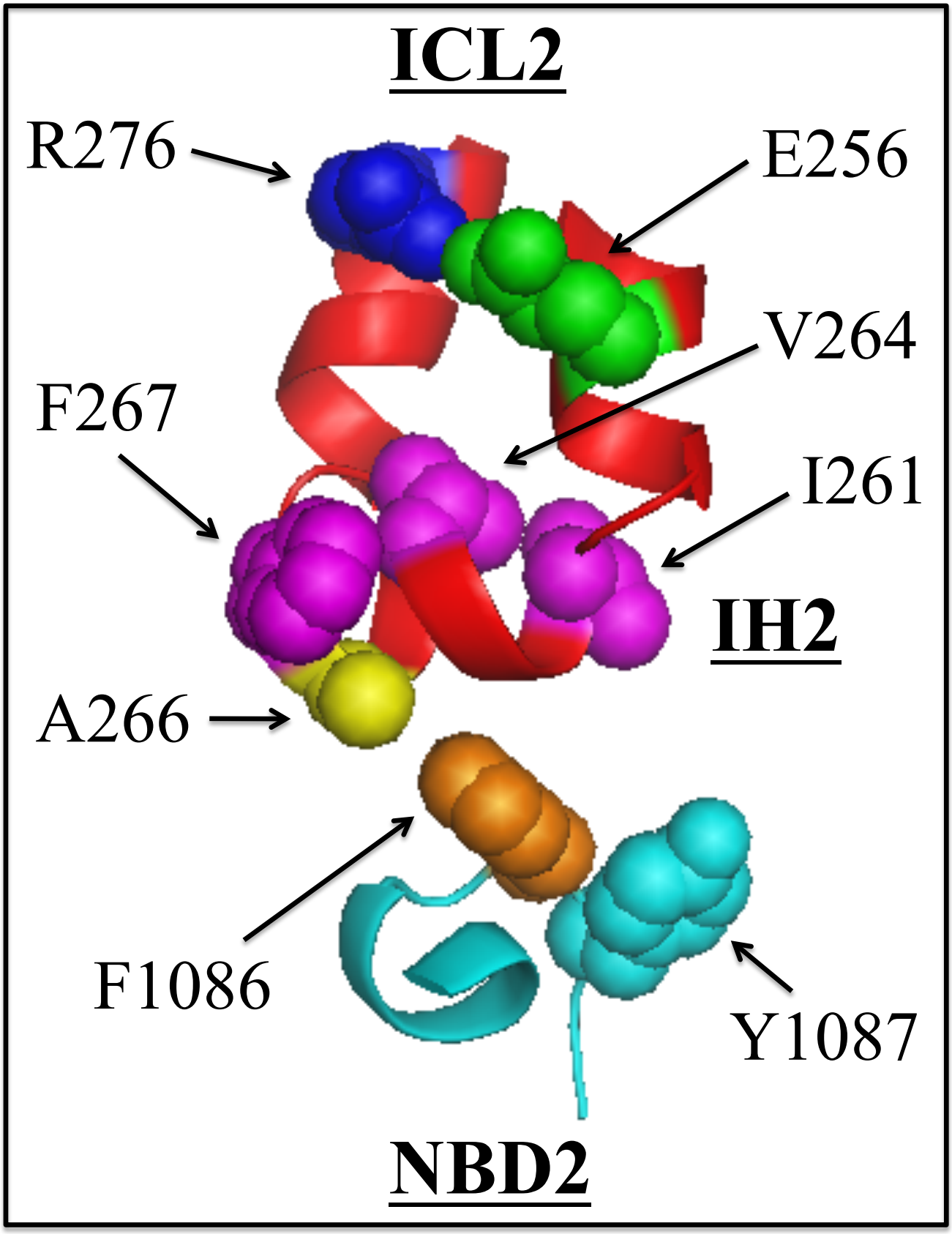

Fig. 7